Origin of Disturbances in Cocurrent Gas-Liquid Packed Bed Flows

D. A. Krieg, J. A. Helwick, P. O. Dillon, and M. J. McCready
Dept. of Chemical Engineering, University of Notre Dame, Notre Dame, IN 46556

Visual, video, pressure, and conductance techniques were used to study time-varying disturbances in cocurrent flow in packed beds with vertical and horizontal columns. It is found that the trickle-pulse transition, as defined in previous studies, corresponds to conditions where traveling disturbances finally become measurable, not the conditions at which infinitesimal disturbances begin to grow. Observations demonstrate that even if the liquid and gas are uniformly distributed initially, segregated, vertical flowing regions with higher or lower than average liquid holdup form after a short distance. Horizontal packed bed experiments, designed to study how regions of differing liquid holdup interact, indicate that the first type of disturbance is infiltration of gas into the liquid region. A simple model suggests that infiltration occurs if the pressure drop exceeds a value necessary to push gas through liquid-filled pores. Once infiltration is significant enough to form a third "bubbly" phase, traveling wave instabilities form and grow into pulses if sufficient column length is available. A three-layer Kelvin-Helmholtz stability model is used to interpret the growth of disturbances in horizontal flows. Video observations of small-scale events in the bed failed to detect significant correlations between different regions. Thus it should be possible to describe flow behavior in these systems with volume-averaged equations, as long as the presence of segregated regions is considered. Column diameter or thickness significantly affects the frequency of disturbances.

Introduction

Gas-liquid catalytic reactions, such as hydrotreating of petroleum fractions and oxidation of formic acid in water, and some noncatalytic ones are conducted in cocurrent flow in packed beds. Laboratory versions of these reactors indicate (Weekman and Myers, 1964; Chou et al., 1977) that different flow regimes exist and that, in general, there are spatial and temporal variations of liquid and gas holdup. These hydrodynamic disturbances cause time-varying gas-liquid, liquid-solid, and gas-solid heat and mass transport rates. Time-varying transport rates, which may have widely different frequencies depending upon reactor size, fluid properties, and packing configurations, can interact with the dynamics of the reaction systems and cause significant changes in selectivity and yield (Wu et al., 1994). Consequently, it is important to know the flow regime and the pertinent time scale and strength of fluctuations.

Correspondence concerning this article should be addressed to M. J. McCready.

Weekman and Myers (1964) reported the existence of flow disturbances and noted a difference between trickling, where only mild small-scale disturbances existed, and pulsing, where strong traveling waves occurred. Numerous articles have followed that were intended to predict and interpret the regime transitions or provide predictions of the dynamics of pulsing. [Herskowitz and Smith (1983) and Santos et al. (1991) review this topic extensively]. Tosun (1984) reviews previous flow regime maps and finds that the Carpentier–Favier map (1975) works reasonably well. Ng (1986) gives stability and other criteria for predicting the entire flow map for cocurrent gas-liquid flow in a packed bed similar to the pipe flow case that was done by Taitel and Dukler (1976). Grosser et al. (1988) use averaged equations of motion for uniformly distributed gas and liquid phases and then show that this uniform state becomes unstable for sufficiently severe conditions. The conditions of instability are found to relate to the onset of pulsing. Further studies by this research group (Dankworth et al.,

1990; Dankworth and Sundaresan, 1992) explore nonlinear equations that control the dynamics of pulsing. Kolb et al. (1990), Melli et al. (1990), and Melli and Scriven (1991) provide extensive measurements and analysis for a two-dimensional bed (i.e., two parallel plates with regularly spaced cylinders between them) that is more amenable to rigorous determination of the important physical effects than a bed packed with particles. They provide pictures and quantitative measurements that characterize pore-scale phenomena and show how macroscale behavior evolves from it. Their theoretical analysis, which is based on a network model, gives accurate overall predictions of the two-dimensional bed—but is very computationally intensive, as it includes equations for every passage. A particularly interesting result of their work is that the dominant frequencies of strong fluctuations are about 40–60 Hz. Experiments described below for a much larger three-dimensional bed find a dominant frequency of about 1 Hz.

Gas-liquid flow in a packed bed is a very complex phenomenon and despite previous studies there are many unresolved issues. First among these is that disturbances in a cocurrent flow system will be "convective" (Huerre and Monkewitz, 1985) and thus travel through the device. It is not possible to determine consistently the existence of spatially growing disturbances by defining a transition to "pulsing" as occurring when pulses are observed ("measurable") at say, 0.5 m from the top of the column. While this definition is useful from a practical standpoint (i.e., either we see pulses or we don't and they may affect our reactions), it cannot be used in conjunction with stability theories for convective disturbances. Convective disturbances, if unstable, will grow with distance until they become observable at a point that depends on flow conditions and the strength of the noise present at the inlet. A true consistent definition of transition will be *if* the disturbances are growing, not if they are *measurable* at a particular location. A second issue is the time scale of disturbances. It is significant that the dominant frequency varies by more than an order of magnitude between a 2.2-mm-length-scale device (Kolb et al's two-dimensional column) and a packed bed with a diameter of 7.62 cm. Some insight into the mechanisms that govern the evolution of disturbances and thus determine the time scale of finite sized disturbances is needed. A third issue involves development of a mathematical description of the flow behavior. Grosser et al. (1988) use volume-averaged equations and find some agreement with data. However their predictions do not agree with data presented below. Melli and Scriven (1991) show that a rigorous way of describing the flow in a packed bed is to use a network model that includes all the possible flow paths. This works well for a small two-dimensional bed but it is not clear how to represent a large three-dimensional bed with this technique in a computationally manageable way.

The objectives of this study were to determine the physical processes that control the time scales and magnitude of disturbances that occur in cocurrent packed bed flows. Because an early set of experiments indicated the presence of vertically oriented segregated regions of differing holdup and because Grosser et al.'s (1988) theory could not explain the transition to pulsing or the onset of traveling waves for a 3.5-cp liquid—possibly because of the importance of segregated regions—a horizontal, stratified, cocurrent flow geometry was used. This geometry represents an extreme limit of segregated regions and provides an unambiguous base state for the gas-liquid flow that is steady in time and describable with volume-averaged equations. Experiments in the horizontal column provided the unexpected result that traveling wave instabilities did not arise unless the liquid phase was infiltrated with gas to form a flowing bubbly phase. The traveling waves looked very much like developing pulses; they grew into pulses if enough column length was available. A force balance to describe the infiltration process and a three-layer Kelvin–Helmholtz stability analysis to describe the initiation of traveling waves appear to contain the correct physical mechanisms of the respective processes. They did not always provide accurate quantitative predictions, however. It was originally thought that traveling waves could be traced to an origin as correlated events on a pore scale such as occurred in the two-dimensional experiments of Melli et al. (1990). This motivated close-up video-imaging experiments in a vertical rectangular bed that used an index of reflection-matched liquid to improve resolution. For most situations, these failed to detect correlated events between different pores in the frame even when traveling disturbances occurred. If pore-scale events lead directly to large disturbances, volume-averaged equations cannot capture the process. Consequently, the lack of small-scale structure to the flow suggests that volume-averaged equations could be used to represent the dynamics of these flows. However, the presence of segregated regions where the averaged properties are different needs to be accounted for. One general observation that we made was that the characteristic length scale of the column significantly affects the frequency of the observed fluctuations.

Description of Experiment

Apparatus

A schematic representation of the experimental setup used to investigate the behavior of gas-liquid in packed beds is depicted in Figure 1. The air supply was from the building

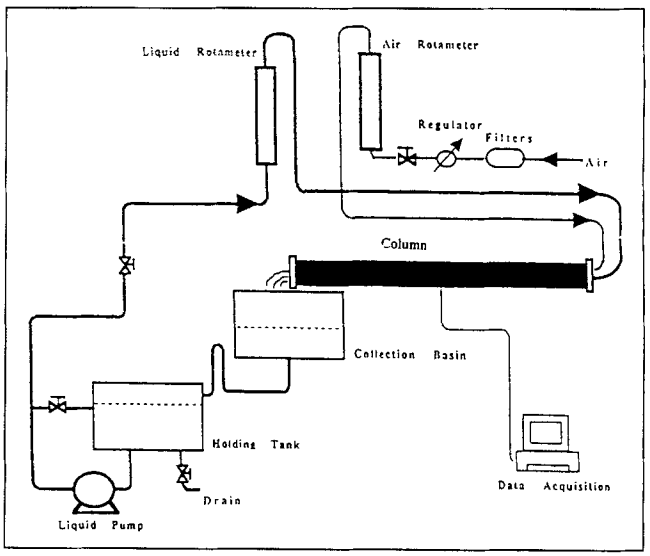

Figure 1. Flow system.

The column may be oriented horizontally or vertically.

compressor and was supplied in a 1/2-in. line. A particulate filter and water and oil traps were present in the line. A two-stage L-Tec pressure regulator was used to reduce the 100-psi (690 kPa) air down to 30 psi (210 kPa); this was connected to an Omega Fl-1500A rotameter. Pressure reduction at the control valve was large enough that the rotameter float fluctuated very little even when the column was pulsing; however, there was no doubt some variation in the flow rate and variation in pressure. The liquids, which were water and glycerin-water solutions of up to 5cp, were supplied from a storage tank using a 1/3-hp (0.25-kW) Eastern Centrichem pump. A Fischer-Porter rotameter was used to measure the liquid flow rate. More details on the supply systems are available in theses by Helwick (1991), Dillon (1992), and Krieg (1994).

Four different clear acrylic columns were used in this work. The vertical, cylindrical column (Helwick et al., 1992) is 1.3 m in length, 1.27 cm in wall thickness, 7.62-cm ID and filled with 0.318-cm nonporous, polished spheres to a packing height of 1.25 m. On top of the packing is a highly porous section of foam, approximately 2.5 cm high, followed by a fine screen acting as a precursor to the packing to ensure uniform distribution of liquid. The entrance section, which sits directly on top of the mesh, is a 10-cm-high monolith "honeycomb" that is designed to have 1/3 of its holes (0.35 cm dia.) with gas flow through it and the rest liquid flow. This design is similar to the one used by Herskowitz and Smith (1978) and provides a uniform distribution of the gas and liquid onto the bed. Four taps for pressure transducers are spaced evenly along the column.

The vertical rectangular column (Dillon, 1992) has dimensions 2.54 cm thick, 15.24 cm wide by 61 cm tall and is packed to a depth of 46 cm with 0.318-cm spheres. The entrance section for the rectangular column was similar to the circular column except that individual passages for air and liquid were constructed from metal and Tygon tubing. This column was operated with the same water and glycerin-water mixtures as the other column or with a 55 wt. % zinc chloride in water solution that matched the index of refraction of the acrylic. The zinc-chloride solution is not perfectly transparent, and it was difficult to match exactly the refractive index of acrylic. However, when the column was filled with liquid and direct lighting was used, it was possible to see clearly several particle diameters into the bed. Backlighting allowed a somewhat fuzzy view through the entire bed. When a gas-liquid flow was occurring, the presence of gas regions reduced the depth of view, but it was still much better than when water or glycerin-water solutions were used.

The two square packed beds are constructed of extruded acrylic and have inside dimensions of 2.54 and 5.08 cm. The 5.08 column is 1.22 m in length and is packed to a length of 1.17 m. At the top of the column, between the fluid inlets and the packing, is 5 cm of highly porous nylon mesh to minimize flow disturbances. Because the flow is intended to start off stratified, a 4-cm-long divider is placed between the gas and liquid inlets to allow for even distribution. A parallel wire conductance probe (McCready, 1986) is situated 61.2 cm from the bottom of the column. Pressure transducer taps are placed in pairs, one for liquid and one for gas, at 30.4 and 92.3 cm from the bottom of the column. Also, single pressure taps are placed on the gas (upper) side of the column at 62.5 and 12.3 cm from the bottom of the column. The 2.54-cm column is also 1.22 m in length and packed to a length of 1.17 m. Three platinum conductance probes are situated at 61 cm, 58.6 cm, and 53.5 cm from the bottom of the column. Four pressure transducers are placed at 12.3, 56.6, 62.5, and 102.5 cm from the bottom of the column. The columns could be oriented either horizontally or declined to an angle of $\pi/4$. Little difference in behavior occurred if the declination angle was $\pi/16$ or less. Consequently, this article considers only the horizontal flow case.

Column operation

Because numerous previous studies have described problems with hysteresis effects, experiments in the vertical columns were started by first increasing the liquid flow to its maximum value and then increasing the gas flow until pulsing occurred, and then operating at these values for a few minutes. This subjected all areas of the packing to gas and liquid flow. Experiments were then done by fixing the liquid flow rate and increasing the gas flow rate. By using this procedure, reproducible experiments were achieved. It is noted that some hysteresis in regime and pressure measurements occurred if the gas flow was reduced as opposed to continuous increase.

The horizontal column was operated in an analogous fashion. Hysteresis effects were present but seemed less significant than for the vertical column.

Pressure measurements

The fluctuating pressure was measured with Omega PX800 Gage pressure transducers that use semiconductor strain gages bonded to a piezoresistive (silicon) diaphragm to measure the pressure with high accuracy and a fast response time. These can detect pressures in the range of 0-10 psig (0-69 kPa) with an accuracy of $\pm 0.1\%$. The signal voltage generated by the transducer is proportional to the amount of supply voltage from its excitation source. To minimize noise, separate DC voltage sources for each probe were used. These were made by placing eight 9-V batteries in parallel. The battery voltage was checked before every run and the probes calibrated as necessary using a water column. The pressure signals were low-pass filtered with a Wavetek analog filter and sampled using MacAdios hardware and software with a Macintosh II computer. A dual-data-acquisition program enables both pressure transducer signals to be sampled simultaneously. The size of each data set ranged from 10,000 to 200,000 data points depending upon the extent of the desired analysis.

Conductance probe measurements

Parallel wire conductivity probes are used to measure the height of liquid in the horizontal column or area occupied by liquid in a cross-sectional area of the tube. These are constructed by stringing two parallel, 28-gauge platinum wires placed 0.635 cm apart. Sodium chloride added to the liquid makes it slightly conducting so that changes in the liquid level can be related to changes in the conductance between the wires. A custom-built electronic transducer/amplifier circuit that operates at 30 kHz is used to measure the change in conductance with time. It provides a continuous voltage out-

put that is proportional to the liquid depth. The complete circuit design for this electronic device is given in a thesis by Jurman (1990). These probes have been used with much success to measure waves in two-phase flows in channels and pipes (Miya et al., 1971; Brown et al., 1978; Koskie et al., 1989). Because there is continuous liquid holdup, this technique cannot be as accurate as it is without packing. However, our experiments indicate that it can detect large disturbances as they travel through the bed. It is noted that when the probes were calibrated, the voltage increased linearly with liquid depth for the entire height of the channel.

Video imaging

Flows in the circular column were observed visually and by using a color S-VHS camera (Panasonic model WV-CL-700). Shutter speeds of 1/250, 1/500, and 1/1,000 s were employed. Various lenses, including a 28-mm, a 50-mm, and a 70–210-mm zoom lens, were used depending upon the length of the column observed. Backlighting was provided by a circular array of eight slide projector bulbs, and red food coloring was added to the liquid. An editing S-VHS VCR (Panasonic AG-7300) was used to play back and analyze the video taken at speeds ranging from slower than real time to a little faster. In addition, it is capable of advancing the videotape one frame at a time. These experiments revealed the presence of traveling liquid-rich regions at conditions where the pressure probes did not detect pulses.

Imaging of the rectangular bed was done using a Kodak Ekta Pro 1000 motion analyzer. Close-up lenses were used so that a typical frame viewed a region that had a nominal size of 1.2 cm and therefore was about 3–4 particle diameters across. A frame is 222 wide by 189 high in pixels, and thus a pixel is about 0.05 mm. Framing rates of 30–200/s were used, but most phenomena occurred with frequencies of about 10–20 Hz. Thus most data were recorded at 60 frames/second. The frames, which are continuous gray, were digitized into 8-bit (256 levels) images and stored on a computer for subsequent image analysis. Full details of the techniques employed and results are given in a thesis by Dillon (1992). One important tool was digital subtraction of background frames (with no flow) from frames that showed important events. Video analysis provided the temporal and spatial scales of the small-scale phenomena—and the similarity of these in the trickling and pulsing regions. Another important result was the lack of localized correlation from pore to pore of small-scale time-varying events.

Theoretical Analysis

Experiments in horizontal beds indicate that the instability that produces large disturbances occurs when there are three phases flowing in the column: a gas phase, a bubbly phase, and a pure liquid phase. It appears that the disturbances originate at the bubbly–liquid interface. To explain the origin of traveling interfacial disturbances that are long compared to packing size, the formulation must include governing momentum equations for the phases and appropriate interfacial boundary conditions. Because the velocity profile should be almost flat within a phase, viscous shear at the interface is likely to be minor, and the wavelength is long compared to the packing size, the instability has many similarities with the Kelvin–Helmholtz model (Chandrasekhar, 1961).

Instability arises in a Kelvin–Helmholtz model when the Bernoulli effect pressure force at the interface, caused by the velocity difference between the phases, is large enough to overcome the stabilizing forces of gravity and surface tension. The Kelvin–Helmholtz model assumes an inviscid flow so that the drag force of the packing, which is usually represented with terms proportional to the first and second powers of velocity (Ergun equations terms), is omitted. Because the Ergun terms always oppose the flow, it is unlikely that they will lead to instability. Stability predictions made with the Ergun terms omitted will be a lower bound on the necessary velocity difference. Note that the base state for stability analysis must be obtained from measurements because the inviscid model cannot predict the depth and velocity of the phases. The primary justification for using the simpler Kelvin–Helmholtz model is that there is uncertainty with expressions for interfacial tension and the Ergun force terms in the bubbly phase so that the result is not expected to match exactly. It is hoped that the stability analysis will provide additional physical insight and rough quantitative agreement.

To model the three-layer packed bed flow, the classic two-layer Kelvin–Helmholtz analysis is extended to include three layers and a finite-sized domain. Another difference is the inclusion of an interfacial tension term that is proportional to displacement. For the present formulation the interface pressure jump term will be

$$-\gamma_i \frac{\partial^2 \eta_i}{\partial x^2} + \sigma_i \eta_i, \quad i = 1,2 \tag{1}$$

where γ_i is the interfacial tension coefficient between the liquid–bubbly ($i = 1$) or bubbly–air ($i = 2$) in the packed bed, η_i is the shape of the two interfaces, x is the flow direction, and σ_i is the interfacial tension defined later in Eq. A10 that is obtained from Grosser et al. (1988) based on drainage. Because it is not clear how interfacial forces will act in this system, results will be presented for γ_i or $\sigma_i = 0$ to show the effect of the different formulation. Derivation of the expression for the eigenvalue relation is a straightforward extension of previous Kelvin–Helmholtz stability results and is presented in the Appendix.

Results

Figure 2 shows a set of pressure tracings taken at a fixed location in the vertical, circular column as a function of time across the observed (at flow rates consistent with the results of Weekman and Myers, 1964) trickle–pulse transition for water as a liquid. The liquid superficial flow rate, L, is held constant, and the gas superficial mass flow rate, G, is varied. A dramatic change in signal is seen as the pulses, which cause large changes in pressure fluctuations, appear. These data suggest that there is a strong qualitative change in the state of the flow associated with the appearance of pulses. However, visual and video observations indicate that organized traveling disturbances similar to pulses are present at G values below the "transition" and in between pulses detected by the pressure probe. It is believed that these traveling waves of liquid have "holes" in them that allow some gas to pass

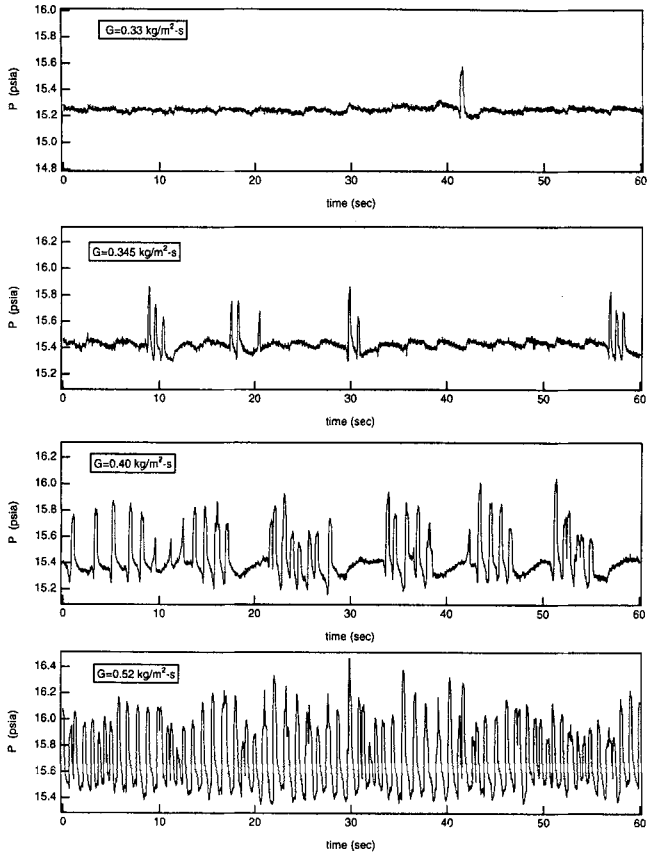

Figure 2. Pressure tracings for $L = 7.9$ kg/m^2·s as a function of increasing G.

If $G < 0.3$, no pulses are detected by the pressure probe. The liquid is water.

through or around, resulting in a lower pressure drop than for pulses. These are analogous to the "pseudoslugs" that Lin and Hanratty (1987) observed in cocurrent gas–liquid pipeline flows. "Pulses" that do not extend across the entire column occur in large industrial columns and were observed in a laboratory column by Christensen et al (1986). To confirm the nature of traveling disturbances that are not pulses, we performed the same experiments with a 3.5-cp glycerin-water mixture which, owing to a higher viscosity, causes larger fluctuations for both trickling and pulsing and allows detection of traveling waves that are not pulses. These data (for the vertical circular column) are shown in Figure 3. At the lowest gas flow rate, highest frequency fluctuations are at about 1 to 1.5/s, and slower variations of about 3 to 5 s are also observable. As G is increased, the 1–1.5-s fluctuations become more pronounced. For $G = 0.277$ kg/(m^2·s), these are easily observed visually as pulses. The frequency spectra of the three tracings are shown in Figure 4. There is no striking change in behavior, only a slight sharpening in the peak. The data in Figures 2, 3 and 4 show that the trickle–pulse transition, as defined in previous studies, corresponds to strengthening of traveling disturbances that exist in the trickling regime and not a qualitative change in the system. Thus, the trickle–pulse boundary is not a traditional hydrodynamic transition and cannot be described with hydrodynamic stability theory as it is normally implemented. If linear stability theory is used to predict traveling disturbances that *may* evolve into pulses, it would predict the conditions of onset (i.e., positive spatial growth) of these disturbances. The point at which they become *detectable* would be at different distances for different conditions because they are spatially growing. Defining a transition as "ability to detect at a specified distance from the inlet," such as is done by Chou et al. (1977), is not consistent, because disturbances that are "undetectable" at 1 m might be strong pulses at 3 m—if the column is long enough.

One last observation from Figures 2, 3, and 4 is useful. Once pulses occur regularly, they have a definable frequency that is about 1/s for both fluids. While this varies somewhat with liquid and gas flow rates (see Kolb et al., 1990, for an extensive discussion), data below suggest that column size is an important variable that controls frequency.

Video observation of the vertical rectangular column was used to examine small-scale fluctuations for conditions both with and without large disturbances present (Dillon, 1992). Events such as bubbling and interface flexing were seen for both conditions, and there was little qualitative difference in these fluctuations for the different regimes. These results suggest that large disturbances are imposed upon a weakly fluctuating background state that does not change qualitatively if pulses are present. Furthermore, we were unable to find spatial correlations of small-scale time-varying behavior that could be implicated in formation of pulses. An interesting result of the video imaging is that time scales for inter-

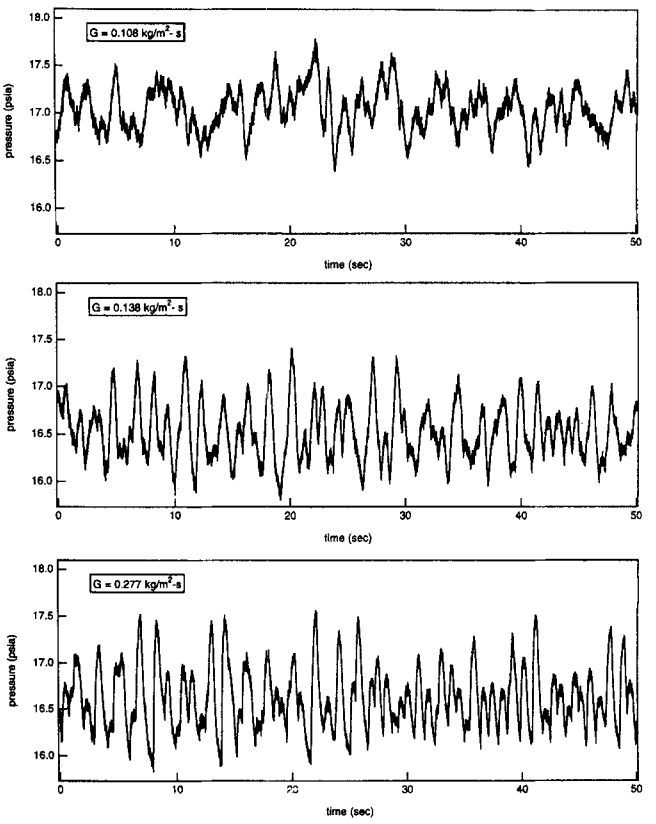

Figure 3. Pressure tracings across the trickle-pulse "transition" for a liquid with $\mu = 3.5$ cp, $L = 3.46$ kg/m^2·s.

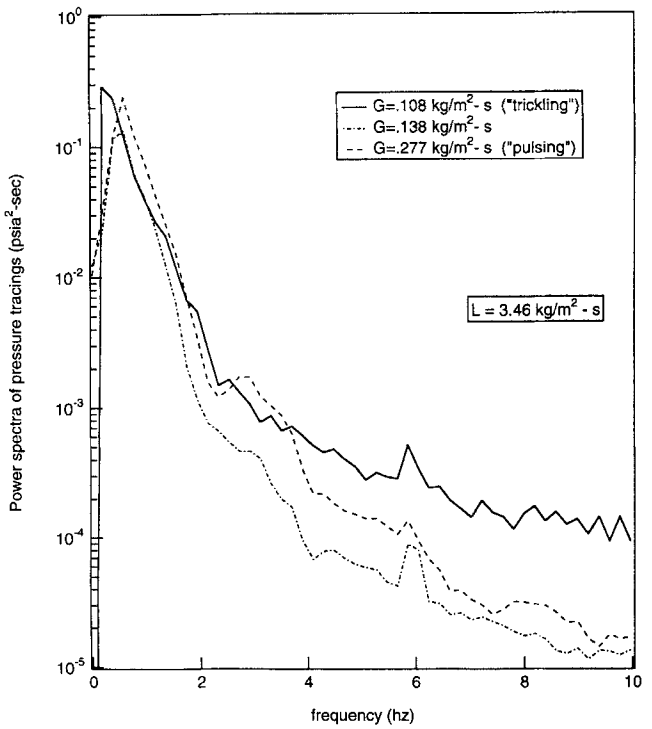

Figure 4. Power spectra of pressure signals for the 3.5-cp solution.

The trickle and pulse spectra have the same dominant frequency and the same shape.

face flexing, bubble passage through pores, flooding of pores, and other small-scale phenomena were about 0.1 to 0.01 s. Time scales for pulses were 0.5 to 1 s, although they seldom extended across the entire long length dimension of the bed in accord with observations of Christensen et al. (1986). For a 2-D bed, Kolb et al. (1990) saw similar events with similar time scales for pore-scale phenomena. However, they noted a distinct peak of 40–70 Hz in their audio spectra when pulsing occurs. The large difference in the time scale of pulses for the two different situations is presumably attributable to the difference in length scales of the thickness of the bed. The present one is 2.54 cm, and Kolb et al.'s is 0.22 cm.

Our video observations in both the rectangular and circular vertical columns show that while the phases are initially uniformly distributed, segregated regions form within a short distance (20–30 cm) from the inlet. We define these regions as roughly vertical passages through the bed that were either usually liquid filled or usually free of liquid. They look similar to the rivulet flow of Lutran et al. (1991), although the ones in our columns are not nearly as well-defined and not as straight. The segregated regions could be clearly seen in the outside of the circular column, and thus could be a wall effect. However, they could be seen inside the column when strong backlighting was used and in the rectangular bed when zinc-chloride solutions were used. Thus, we believe that they exist. In the absence of pressure gradients large enough to force gas through liquid-rich regions (such as the infiltration phenomenon discussed below), it is not obvious how regions of liquid could be broken up once they form. Further evidence of the development of segregated regions is the need for redistributors in large industrial beds. The almost ubiquitous existence of segregated regions leads to the obvious question: How do liquid-rich and gas-rich regions interact? To study this question, the horizontal square columns were employed.

For sufficiently low flow rates, the stable stratified interface did not appear to change with distance or time. The existence of a stable region at low flows would be expected because of gravitational and capillary stabilization. Furthermore, small wavelength disturbances would be impossible because the packing size is 0.318 or 0.636 cm. A stable stratified flow provides an unambiguous base state on which to base stability calculations. Figure 5 compares the pressure drop predicted from the Ergun equation (constants are 150 for linear velocity term and 1.75 for quadratic term) with measurements for a typical run in the horizontal column. Note that U_G is the air superficial velocity based on the actual area of flow for the gas phase, not the entire area of the column. The prediction is obtained by using separate Ergun equations for each phase and adjusting the liquid depth so that the pressure drop in each phase matches. It is seen that for sufficiently slow gas velocity, the agreement is within the accuracy of the experiments. As the gas velocity is increased, the pressure drop increases faster than the prediction. This occurs as the flow becomes disturbed. The first disturbance is the bubbling of gas down through liquid-filled pores in the region occupied by the liquid phase. At onset, a gas path will be one or two spheres deep and travel five or six sphere diameters in length. As the gas flow increases, the depth and length increase. At some point, which was not well-defined, the disturbed region grows with distance also and forms what is essentially a third phase. This bubbly phase travels with a velocity intermediate between the gas and liquid and has a density that is also intermediate between the two. This phase is essential in the formation of waves since they are not observed if it is not present.

Figure 6 shows a typical regime map for the horizontal column. The superficial gas and liquid velocities are based on the liquid height near the beginning of the column before

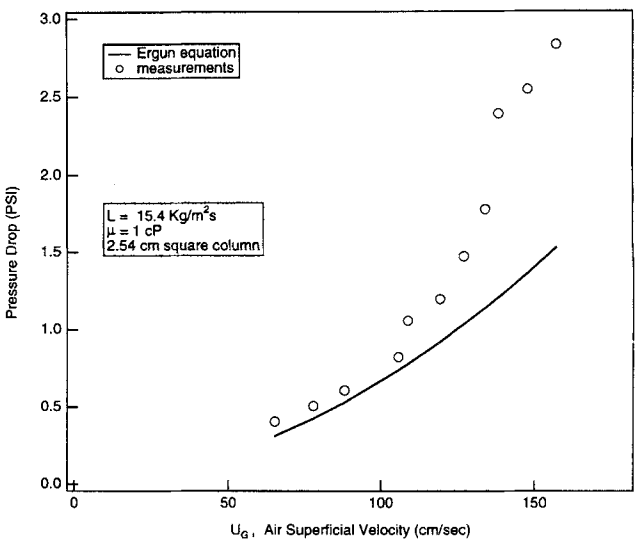

Figure 5. Measured vs. predicted pressure drop for two-phase flow in a packed bed.

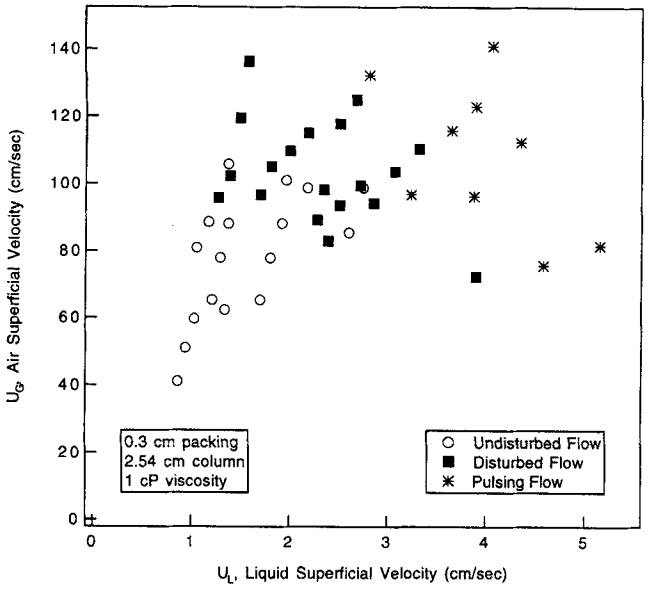

Figure 6. Regime map for the 2.54-cm-square horizontal column.

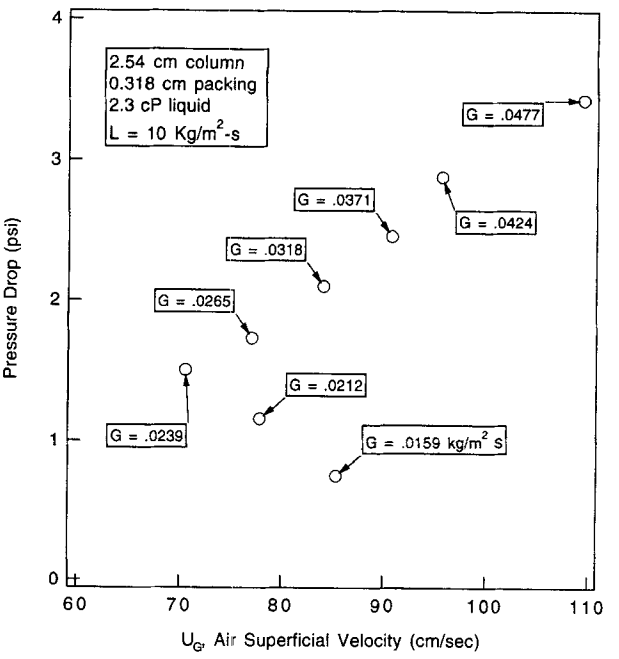

Figure 7. Pressure drop increases with increasing total gas flow, but the gas volumetric flow/gas flow area ratio initially decreases as liquid depth is reduced.

disturbances occur. Because of the number of variables, it is not likely that data for different fluids could be collapsed into a single two (dimensionless) parameter plot. No such plot has been found for the gas–liquid pipe flow situation for either vertical or horizontal flow or for the vertical packed bed. We note that data for the 2.54 and 5.08-cm columns are similar and that liquid viscosity has a minor effect. For all of our data with 0.318-cm spheres, a line between $U_G = 100$ cm/s and $U_L = 3$ cm/s is close to the undisturbed–disturbed boundary. For 0.636-cm spherical packing, a large region of undisturbed flow exists above this line. The reason for this is that larger packing allows a larger gas flow with a lower pressure drop than smaller packing; a sufficiently large pressure drop is needed to force gas into liquid-filled pores.

Figure 7 shows an interesting feature of two-phase cocurrent horizontal flows. The experiment shown here was a measurement of the average pressure drop for fixed liquid flow rate as the gas flow rate was monotonically increased. The data points are labeled with the gas flow rate, which is always increasing. The gas flow rate/area (U_G) decreases for the lowest pressure drops, even as the total gas flow rate is increased and the liquid flow rate is held constant. This initial decrease occurs because the less viscous gas can force the liquid to occupy a smaller flow area, thus leading to a smaller increase in pressure drop than would occur if the liquid did not get pushed out of the way. At some point this no longer occurs and the gas superficial velocity increases. If the gas flow rate is decreased at some point in the experiment, the pressure drop and liquid height do not exactly match the values obtained from monotone gas increase. However, the difference was typically less than 5% so this hysteresis is not a major issue. The shape of the curve in Figure 7 was observed for all horizontal flow experiments, but the onset of disturbances occurred in both the positive and negative slope regions for different experimental conditions.

Interfacial waves were observed to grow into pulses. Figure 8 shows how the conductance and pressure probe measurements compare for conditions where the 2.54-cm horizontal column is pulsing. The height tracing shows pulses more clearly and gives a better idea of how long a pulse lasts. The pressure is higher than baseline until the pulse leaves the column. The conductance probe returns to baseline once the pulse has passed it. Because the pulses are not pure liquid, the measured height does not read 2.54 cm even when the pulses occur and extend the entire height of the column.

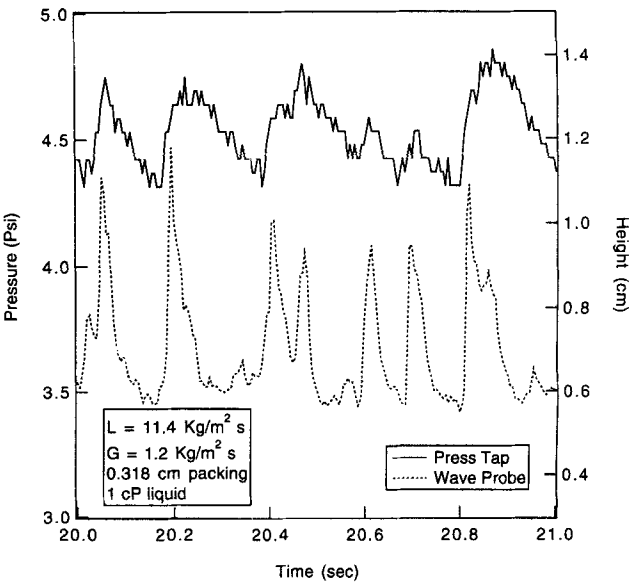

Figure 8. Pressure probe vs. wire probe tracings.

Note that the front of tracings line up well. The pressure stays elevated until the pulse leaves the column and is therefore wider than the wire probe that measures liquid concentration locally.

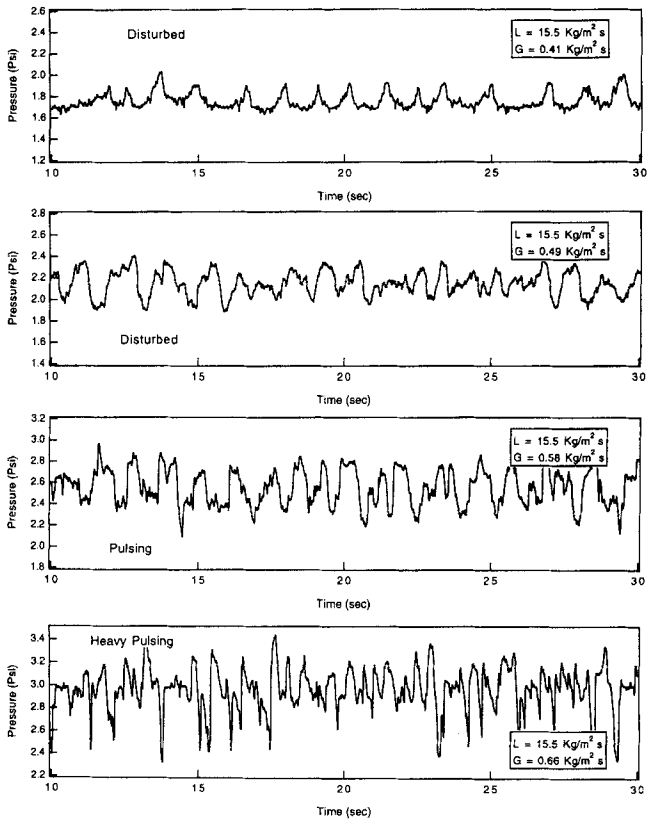

Figure 9. Pressure tracings as a function of gas velocity ranging from mild waves to pulses.

Figure 9 shows pressure tracings from the 2.54-cm horizontal column for conditions from the appearance of weak waves to strong pulses. Waves were observed to form at a point that depended on flow conditions and then once formed, they increased in amplitude until they reached to the top wall or ran out of column length. These have the standard behavior for a convective disturbance. Waves were observed only after a bubbly phase had developed. As will be discussed below, this seems to be because the velocity difference that could be achieved between the pure phases was never large enough to overcome stabilization. However, the presence of a bubbly phase, which is much more dense than the gas phase and travels faster than the liquid phase, can lead to an instability.

Other than the transition point to pulsing, a useful feature of pulses is their frequency. A problem with comparing measurements of frequencies for pulses in packed columns or slugs in pipes is the effect of the air supply system on this property. While a flow system may provide a nominally constant flow rate, the large fluctuations in pressure associated with pulses or slugs will cause fluctuations in the gas flow rate. This in turn leads to differences in the speed of propagation and therefore frequency. An extreme example would be a system that approximates a constant pressure drop and would reduce the gas flow as the disturbance started to grow; this would likely kill the disturbance. A perfect system would have such a large pressure drop at the control valve that flow remained absolutely constant. This would not completely solve the problem for a compressible fluid unless the average pressure was much larger than the fluctuation. In our vertical column, pressure fluctuations are about 1–2 psi (7-14 kPa), which is significant compared to average pressure, so that perfect conditions are not realized. However, because our different experiments have the same air and liquid supplies, we have a good basis for comparison. Figures 2, 3, and 4 show that the frequency of the 7.62-cm circular column is about 1/s. Figure 10a shows power spectra for the wave probe in the 2.54-cm square column for fixed liquid flow rate at increasing gas flow rate. Experiments start at the gas flow rate for which the first disturbances are observed. The peak is broad and changes from run to run, but most of the energy is in the range of 2–10 Hz. Figures 10b and 11a show the same measurements for the 5.08-cm-column at two different liquid flow rates. The frequency is lower, most of the energy is confined below 2 Hz, and the liquid flow seems to have little effect. When the packing size was doubled, however, the frequency spectra change significantly. Significant energy is present out to 15 Hz. Note that the gas flow rates are 5–10 times higher for the larger packing size. This is because pressure drop is lower for larger packing, and thus higher gas flow rates are needed to start the infiltration process. The substantially higher gas velocity probably leads to higher frequency waves.

Discussion

Large disturbances in vertical columns

Our interpretation of experimental observations suggests two primary claims that differ from previous studies and mo-

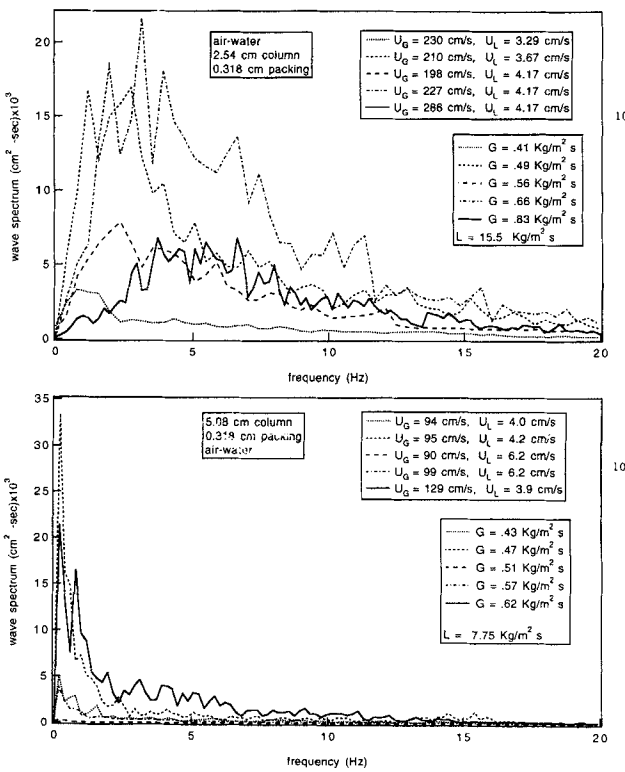

Figure 10. Spectra of wave tracings for 2.54 and 5.08 columns for conditions where disturbances form.

The larger column has lower frequency disturbances.

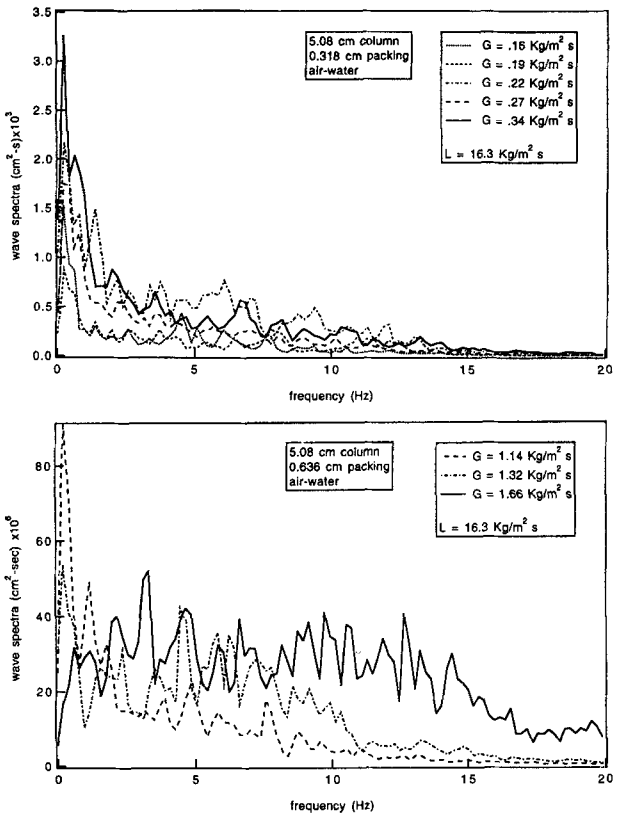

Figure 11. Demonstration of packing size on wave frequency.

Much larger low-frequency disturbances are present for the smaller packing size shown in the top plot as compared to the bottom figure.

tivate the present work. The first is that initially well-distributed phases become less uniform within a short distance and that this inherently heterogeneous state is the proper base state for interpreting formation of strong disturbances. The second observation is given in Figures 3 and 4 (and supported by many visual and video observations for water as the liquid). It is that traveling liquid-rich disturbances, which may not have large pressure fluctuations associated with them, exist at conditions too moderate or distances too short for pulses to form.

If linear stability based on the volume-averaged equations (Grosser et al., 1988) is used to interpret the data of Figure 3 where $L = 3.46$ kg/m^2·s, instability is predicted at $G = 0.8$ kg/m^2·s. Experiments show that fluctuations exist at 0.108 kg/m^2·s and full pulses are present within the column at 0.138 kg/m^2·s. Thus there is disagreement. Further, because Grosser et al.'s (1988) predictions agree with the trickle–pulse transition as normally defined for water as the liquid, but our observations are that traveling waves similar to pulses are present below this transition, there is further disagreement between their theory and our observations. Stability theory, as used by Grosser et al. (1988), should predict the onset of any traveling disturbances that are large compared to pore scales. It is noted that the more elaborate analysis of Dankworth et al. (1990) suggests a slight modification of the boundary, but not enough to explain the discrepancies.

The question that arises is: How should these flows be modeled? Melli and Scriven (1991) used a model that included all flow passages in their two-dimensional bed. Because this required 25 hours of Cray X-MP time, they mention that extending this calculation to full-sized, three-dimensional beds would require computational power far beyond what is currently available. While it is possible that some type of massively parallel model could be contrived to take advantage of new computer architectures, representation of gas–liquid flow in a packed bed with averaged equations is probably necessary for at least the short term. Because we were unable to find (Dillon, 1992) evidence of correlated fluctuations between different pores in a region that could be linked to formation of large disturbances, use of volume-averaged equations seems justifiable for describing disturbances that are much larger than pore scale. The discrepancy between experiments and the predictions of the volume-averaged equations could occur because the phases are not uniformly distributed. To verify this point, Grosser et al.'s (1988) model would have to be reformulated to include a gas-rich phase and a liquid-rich phase coupled through interfacial boundary conditions. If this is done, the primary difference from the Kelvin–Helmholtz model described earlier would be the inclusion of the Ergun equation force terms on stability. It would also be necessary to determine for the vertical bed how many layers of phases need to be included and what their properties are.

Instability in horizontal beds

Figure 10 shows values of U_L and U_G, obtained from the flow rates and areas based on the average location of the gas phase. When a two-layer Kelvin–Helmholtz model is used for horizontal columns, instability is predicted for a gas–liquid velocity difference of 879 cm/s for equal depths; the difference can be as low as about 724 cm/s if the gas phase is confined to a depth of 2 particles. The data show that the largest velocity difference is only about 280 cm/s! Velocity differences never approach 700 cm/s for any of our experiments. As mentioned before, a more elaborate model would include the additional Ergun force terms in the momentum equation. It is difficult to see how this would enhance instability because these terms are resistive. Viscous effects near the phase boundary could be destabilizing, but the presence of particles limits the viscous contact between phases. Thus it is unlikely that the two pure phases will become unstable. The observed infiltration of gas into liquid appears to be needed to explain the onset of instability.

Our visual observations indicate that gas is forced down and through liquid-filled pores. Forcing for this process must come from the average pressure drop and the dynamic pressure of the moving gas. The forces opposing this should be gravity (if the column is horizontal) and capillary pressure. An equation that balances these forces, derived in the Appendix, is

$$-\Delta P + \frac{\rho_G U_G^2}{2} = \epsilon(\rho_L - \rho_G) g \Delta h + 2\frac{\gamma}{r_h} \qquad (2)$$

where ΔP is the pressure change over a specific infiltration length, Δh is the infiltration depth, and r_h is the radius of curvature for the interface within the packing, ϵ is the void fraction, ρ_L and ρ_G are the densities of the liquid and gas, γ is the air–liquid surface tension coefficient, and g is the grav-

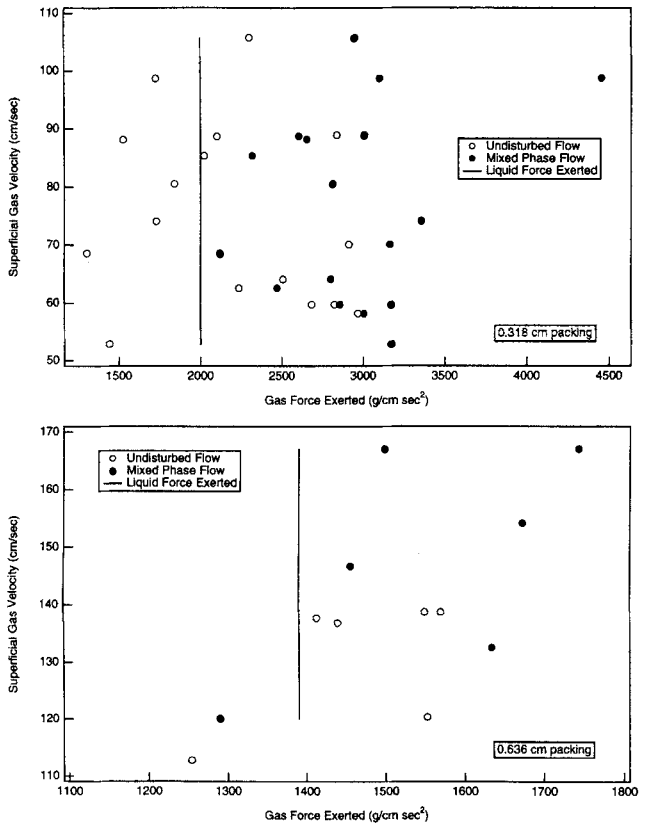

Figure 12. Infiltration equation vs. experiments.

itation constant. If infiltration is predicted, it is necessary to obtain length scales for infiltration from experiments. Typical numbers from observations are a depth of two packing diameters and a length of 2 cm. The radius of curvature is estimated to be 1/2 of the radius of the packing. For 0.318-cm spheres, the gravity term is about 1/10 the size of the capillary term and is thus about 1/5 for 0.636-cm spheres. Figure 12 shows experiments where U_G is plotted versus the left side of Eq. 2; the right side of Eq. 2 is plotted as a line. The lines are expected to be rough bounds on infiltration. Equation 2 seems to be a lower bound on infiltration because only one data point lies to the left of the line. This is admittedly a crude model and further scrutiny is warranted, perhaps using a regular packed array.

It is noteworthy that the pressure drop for infiltration is quite high. Using data from Storck et al.'s (1986) Figure 11, it is found that a typical pressure change in trickling flow over 2 cm would be about 50–500 g/cm·s^2. It is not until the pulsing regime where average pressure drops are large enough for the infiltration mechanism to be predicted to be important. The large pressure drop needed for infiltration to occur might explain why trickle flow has such a strong tendency to form segregated regions. Of course the results do not mean that bubbling does not occur in trickling flow. It certainly does. They mean that the observed bubbling is not predicted to occur by gas displacing liquid in regions of continuous liquid. The results suggest that regions of almost static liquid holdup, which have been implicated in catalyst deactivation or formation of overheated regions, can be reduced by operating at increased pressure drops.

In the present experiment, once bubbling occurred, or sometimes after a slight increase in gas flow rate, the bubbly region grew in thickness with distance. This is consistent with the model because the pressure change does not decrease and there is plenty of air available in the bubbly phase to participate in further infiltration. It is likely for a very deep liquid phase that this layer would not increase all the way to the bottom because of the combined effects of gravity and lack of enough gas phase.

Once a well-defined bubbly phase was present, disturbances always began to form. To check the agreement with the three-layer Kelvin–Helmholtz model, the density and velocity of the bubbly phase are needed. Measurements of amount of liquid in the bubbly phase, obtained from conductivity measurements and mass balance, indicate that it is about one-half liquid. If this is the case, the effective density of the bubbly phase is about 0.175 g/cm^3, because the density of pure water in a packed bed with a 0.37 void fraction is 0.37 g/cm^3. For this difference in density, the Kelvin–Helmholtz model predicts a required velocity difference of only 18 cm/s for instability. It varies only slightly for different depths and gas phase velocities. It is seen from Figure 10a that typical gas velocities are 200 cm/s and liquid velocities are 3–4 cm/s. The bubbly phase must be somewhere in between, so it seems likely that the required velocity difference can always be attained. Figure 13 shows the predicted wave speed (made dimensionless with the bubbly phase velocity) and growth rates (made dimensionless with the channel height and bubbly phase speed) for conditions similar to those shown in Figure 10a. The interfacial tension between the bubbly and the liquid phase, γ_1, was varied because this value is uncertain. The values for σ_i are set to 0, and the value for γ_2, which did not affect the results very much, was held constant at 72 dyne/cm. The speed of the bubbly phase, 22.9 cm/s, was chosen somewhat above the minimum 21.9 cm/s so that the effect of γ_1 could be shown. The first important point is that the dimensionless wave speed is about 0.6 (of the bubbly phase speed) when waves are unstable. This is consistent with the idea that unstable waves are growing at the interface between the pure liquid and bubbly phases. The effect of interfacial tension is to change the cutoff wave number. Note that long waves are most unstable for all values of γ_1. For $\gamma_1 = 72$, all waves longer than about 10.6 cm with frequencies lower than 1.2 Hz are unstable. Because longer waves have a larger growth rate, the wavelength is too long and the frequency is too low to match the data. However, the frequency of the disturbances is very sensitive to the speed of the bubbly phase. For $\gamma_1 = 72$ dyne/cm, $U_2 = 30$, 50, and 70 cm/s, and with the other variables held at their values for Figure 13, the growth curve has a peak at finite wave number with most unstable wavelengths of 21.3, 5.3, and 3.2 cm that correspond to frequencies of 0.83, 4.9, and 9.4 Hz, respectively. Thus, it would be easy to get agreement with data. However, because we don't know the speed of the bubbly phase, there does not seem to be a point to picking values to get better agreement.

Figure 14 shows stability calculations for $\gamma_i = 0$ and $\sigma_2 =$ 15,597 dyne/cm^3, the values predicted by the drainage model used by Grosser et al. (1988) for an air–water interface and $\sigma_1 = \sigma_2/2 = 7{,}799$ dyne/cm^3, because the bubbly–water interface should have a lower effective value. The large value of σ_2 causes a greater value of U_2 to be required for instabil-

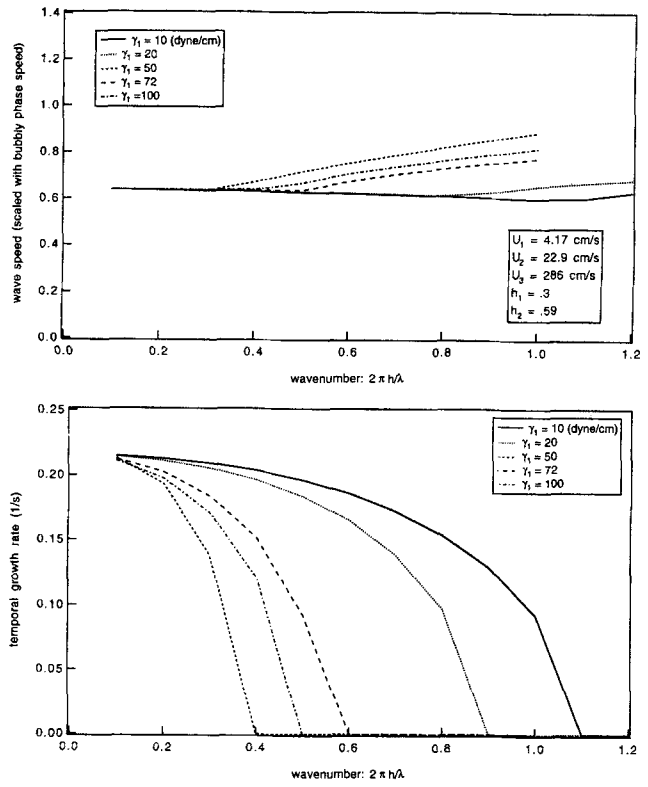

Figure 13. Wave speed and growth curve for 3-layer Kelvin–Helmholtz model.

Conditions were chosen to simulate Figure 10a.

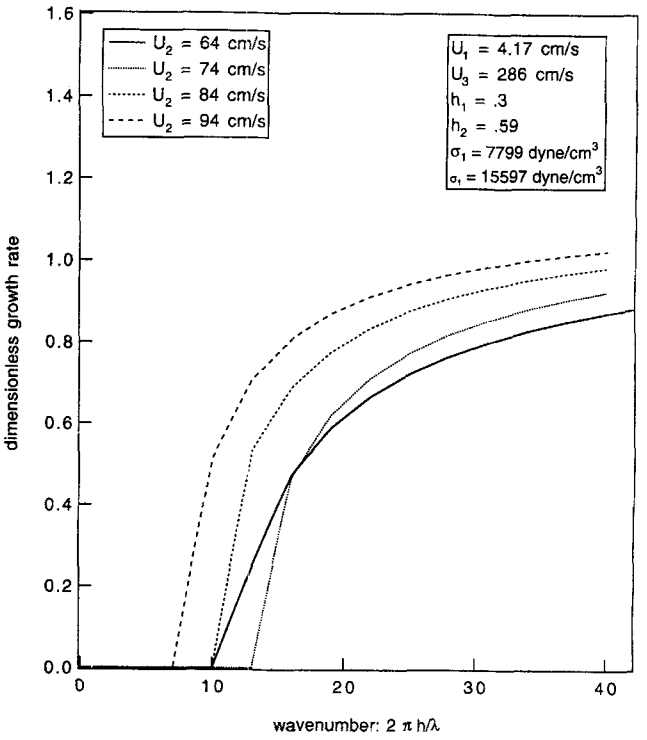

Figure 14. Linear stability predictions for conditions of Figure 10a.

It uses a capillary-restoring force that does not depend on wave number.

ity at wave numbers less than 10 in Figure 14 than for Figure 13. All of the growth curves increase to the right and do not come down. If the value of σ_i is reduced by a factor of 10, the curves move to the left by about 5 wave number units but have the same shape and magnitude. The lack of a curvature effect, which prevents the appearance of a k^2 factor in the interfacial tension restoring force, is the primary difference between Figures 13 and 14. It is not clear which of these two models is more realistic. The data do not show evidence of high wave number modes as predicted for finite σ_i with $\gamma_i = 0$, but these may be mitigated by nonlinear effects. To resolve this issue, an experiment that measures dynamic surface tension as a function of interface curvature is needed.

Large disturbances in vertical beds

It is possible to interpret instabilities in vertical columns with the model for horizontal beds. Because the phases are initially well-distributed, infiltration will not be necessary for the onset of instability in vertical beds. Essentially the bed is bubbly everywhere and as segregation of the phases occurs, the liquid holdup becomes a function of position. If conditions are sufficiently severe, regions of different liquid holdup and velocity will interact, causing the onset of disturbances. In this case the sole restoring force is interfacial tension. If disturbances form, they could grow with distance, picking up more liquid until they form pulses; remain as weak traveling waves; or die out as they move to regions of different liquid concentration. Because there is no quantitative information about the size, velocity, and holdup of different regions of the beds, it is not possible to make any quantitative predictions at this time.

Mechanism of pulse formation

Even though it is difficult to make quantitative predictions of pulse formation, the mechanisms that lead to traveling waves and pulses seem clear from the present experiments and the calculations of Melli and Scriven (1991). If a growing, traveling instability develops between two regions of different velocity and holdup, it will begin to carry liquid with it as it grows in amplitude. As this blob of water is pushed through the column, it is continuously fed with liquid from existing holdup in the bed because it is traveling faster than the average liquid velocity. At the same time, gas is accelerated around the blob, as calculations of Melli and Scriven (1991) show clearly for a 2-D bed. This causes a low pressure region around the edges of the blob that draws liquid from the blob into the gas space (by essentially the same mechanism as waves form in a horizontal bed). The gas flow may also sweep additional liquid into the space that the gas is occupying. If a pulse is growing, its velocity will continue to increase as more gas is blocked off and a larger pressure rise develops behind the pulse. The pulse will also leave some liquid behind so it is necessary for sufficient liquid holdup to be present in the bed to support growth or at least maintenance of the blob. Otherwise, the gas will force holes through the middle of the pulse as the pressure drop increases and the blob thins due to liquid being sucked into the gas bypass region at the edges of the blob.

Pulse time period

The importance of the air supply system to the frequency of large disturbances was discussed earlier, and Kolb et al. have discussed the effect of gas and liquid flow rates. The pulsing frequency varies by over an order of magnitude between the 0.22-cm 2-D column of Kolb et al. (1990)—40–70/s, and the present 7.62-cm column—1/s. If packing size is held constant, the results in Figures 10 and 11a indicate that the frequency of the 5.08 horizontal column, < 1/s, is substantially lower than the 2.54-cm column, 2–5/s. Thus there seems to be a decrease in pulse frequency with increasing column size. It is tempting to look to the linear stability analysis of the horizontal flow for the origin of the frequency effect. The preceding discussion (in the "Instability in Horizontal Beds" section) demonstrates the sensitivity of peak frequency on the bubbly phase velocity as predicted from linear analysis. Figure 10 indicates that typical U_3 values for the 2.54-cm column are 200 to 300 cm/s and the 5.08-cm column is about 100 cm/s. However, note that there is no consistent trend nor a large change in the frequency of the peak for the different runs in Figure 10a. Figure 11a has higher liquid flow rates and much lower gas flow rates, and there is still no significant change in frequency. While it is possible that the waves were at different stages of development for the two different columns, it is hard to ascribe the differences in frequency to linear effects. Consequently, because the dominant frequency changes little with flow rates for either column size, including the vertical column, it is likely that the observed frequency is a characteristic of the size of the column. This result is consistent with the notion that there must be some relation between height (or width) and length of large disturbances. It is reasonable to assume that a pulse that is 5 cm wide would not be as long as one that is 100 cm wide. If the column is very long, it is not clear to how wide pulses could grow. However pulses cannot be wider than the column diameter. For equal superficial velocities, a larger conduit diameter would tend to have at least some wider, and longer pulses thus have a lower frequency of pulsing. This property suggests that it should be possible to "tune" pulse frequency in a large reactor by changing the internals to smaller pipes of a particular size. Data on the effect of packing size in Figure 11b require that this statement be qualified. For the horizontal column, much higher gas velocities are necessary to achieve the pressure drop required to make the instability process occur. The increased velocity seems to be responsible for higher frequency fluctuations. However, for a vertical column where infiltration is not occurring, the instability process that leads to pulsing may not depend strongly on packing size. Rao and Drinkenburg (1983) found only a slight effect on pulse frequency for 0.6-cm Raschig rings vs. 0.3-cm spheres. In any case, questions remain as to the effect of packing size on pulsing.

Conclusions

Traveling waves of high liquid holdup, similar to pulses, are present in the trickling region so that the transition from trickling to pulsing corresponds to only a quantitative change in the strength of these waves and not a hydrodynamic transition. Because uniformly distributed phases form segregated regions of higher and lower liquid holdup within a short distance from a distributor, it is probably necessary to study this heterogeneous state to interpret the origin of traveling waves and pulses. Video observations of pore-scale phenomena fail to reveal significant local correlations of time-varying events. Thus the use of volume-averaged equations to predict large-scale phenomena in packed beds is probably justified. However, these models need to be formulated to include interactions between high-liquid and low-liquid regions rather than averaging over the entire bed. Experiments using a horizontal, gas–liquid packed bed flow to examine an extreme limit of segregated regions show that the flow will be stable until gas infiltration into the liquid-filled region occurs and forms a (third) bubbly phase. Infiltration seems to occur when the pressure drop is large enough to overcome the effects of gravity and surface tension within the liquid phase. A three-layer Kelvin–Helmholtz stability analysis predicts that no interfacial instability will arise if a bubbly phase is not present and that the flow is always unstable once the bubbly phase forms. Experiments in different size columns and with different packing sizes demonstrate a strong effect of the frequency of large disturbances on column length scale and an uncertain effect of packing size.

Acknowledgment

This research was supported by Amoco Oil Company.

Notation

g = gravity constant
h = channel height, either 2.54 or 5.08 cm
h_1 = height of liquid phase
h_2 = location of liquid phase–bubbly phase interface
U_L = liquid superficial velocity defined as liquid volumetric flow rate/area of liquid flow
U_j = average velocity of phase j (cm/sec)
y = direction normal to gas–liquid interface
∇ = gradient operator

Subscripts

i = refers to liquid–bubbly $i = 1$, or bubbly–gas $i = 2$ interfaces
j = liquid phase, $j = 1$; bubbly phase, $j = 2$; or gas phase $j = 3$

Literature Cited

Brown, R. C., P. Andreussi, and S. Zanelli, "The Use of Wire Probes for Measurement of Liquid Film Thickness in Annular Gas-Liquid Flows," *Can. J. Chem. Eng.*, **48**, 52 (1978).

Chandrasekhar, S., *Hydrodynamic and Hydromagnetic Stability*, Oxford Univ. Press, Oxford, (1961).

Charpentier, J., and M. Favier, "Some Liquid Holdup Experimental Data in Trickle-Bed Reactors for Foaming and Nonfoaming Hydrocarbons," *AIChE J.*, **21**, 1213 (1975).

Christensen, G., S. J. McGovern, and S. Sundaresan, "Cocurrent Downflow of Air and Water in a Two-Dimensional Packed Column," *AIChE J.*, **32**, 1677 (1986).

Chou, T. S., F. L. Worley, and D. Luss, "Transition to Pulsing Flow in Mixed-Phase Cocurrent Downflow through a Fixed Bed," *Ind. Eng. Chem. Process Des. Dev*, **16**, 424 (1977).

Dankworth, D. C., I. G. Kevrekidis, and S. Sundaresan, "Dynamics of Pulsing Flow in Trickle-Beds," *AIChE J.*, **36**, 605 (1990).

Dankworth, D. C., and S. Sundaresan, "Time Dependent Vertical Gas-Liquid Flow in Packed Beds," *Chem. Eng. Sci.*, **47**, 337 (1992).

Dillon, P. O., "A Study of Time-Dependent Gas-Liquid Flow in a Packed Bed Using Digital Image Analysis Techniques," MS Thesis, University of Notre Dame, Notre Dame, IN (1992).

Drazin, P. G., and W. H. Reid, *Hydrodynamic Stability*, Cambridge Univ. Press, Cambridge, England (1981).
Grosser, K., R. G. Carbonell, and S. Sundaresan, "Onset of Pulsing in Two-Phase Cocurrent Downflow through a Packed Bed," *AIChE J.*, **34**, 1850 (1988).
Helwick, J. A., P. O. Dillon, and M. J. McCready, "Time Varying Behavior of Concurrent Gas-Liquid Flows in Packed Beds," *Chem. Eng. Sci.*, **47**, 3249 (1992).
Helwick, J. A., "The Study of the Time-Varying Behavior of Gas-Liquid Cocurrent Flow in a Packed Bed," MS Thesis, University of Notre Dame, Notre Dame, IN (1991).
Herskowitz, M., and J. M. Smith, "Liquid Distribution in Trickle-Bed Reactors, Part I: Flow Measurements," *AIChE J.*, **24**, 439 (1978).
Herskowitz, M. and J. M. Smith, "Trickle-Bed Reactors: A Review," *AIChE J.*, **29**, 1 (1983).
Huerre, P., and P. A. Monkewitz, "Absolute and Convective Instabilities in Free Shear Layers," *J. Fluid Mech.*, **159**, 151 (1985).
Jurman, L. A., "Interfacial Waves on Sheared, Thin Liquid Films," PhD Thesis, Univ. of Notre Dame, Notre Dame, IN (1990).
Kolb, W. B., T. R. Melli, J. M. de Santos, and L. E. Scriven, "Cocurrent Downflow in Packed Beds. Flow Regimes and their Acoustic Signatures," *Ind. Eng. Chem. Res.*, **29**, 2380 (1990).
Koskie, J. E., I. Mudawar, and W. G. Tiederman, "Parallel Wire Probes for Measurement of Thick Liquid Films," *Int. J. Mult. Flow.*, **15**, 521 (1989).
Kreig, D. A., "Stratified Flow in a Packed Column," MS Thesis, Univ. of Notre Dame, Notre Dame, IN (1994).
Lin, P. Y., and T. J. Hanratty, "Detection of Slug Flow from Pressure Measurements," *Int. J. Multiphase Flow*, **13**, 13 (1987).
Lutran, P. G., K. M. Ng, and E. P. Delikat, "Liquid Distribution in Trickle Beds: An Experimental Study Using Computer-Assisted Tomography," *Ind. Eng. Chem. Res.*, **30**, 1270 (1991).
McCready, M. J., "Spectral Behavior of Capillary Waves in Gas-Liquid Flows," *Phys. Fluids*, **29**, 2836 (1986).
Melli, T. R., J. M. de Santos, W. B. Kolb, and L. E. Scriven, "Cocurrent Downflow in Networks of Passages. Microscale Roots of Macroscale Flow Regimes," *Ind. Eng. Chem. Res.*, **29**, 2367 (1990).
Melli, T. R., and L. E. Scriven, "Theory of Two-Phase Cocurrent Downflow in Networks of Passages," *Ind. Eng. Chem. Res.*, **30**, 951 (1991).
Miya, M., D. E. Woodmansee, and T. J. Hanratty, "A Model of Roll Waves in Gas-Liquid Flow," *Chem. Eng. Sci.*, **26**, 1915 (1971).
Ng, K. M., "A Model for Flow Regime Transitions in Cocurrent Downflow Trickle-Bed Reactors," *AIChE J.*, **32**, 115 (1986).
Panton, R. L., *Incompressible Flow*, J. Wiley, New York, p. 675 (1984).
Rao, V. G., and A. A. H. Drinkenburg, "Pressure Drop and Hydrodynamic Properties of Pulses in Two-Phase Gas-Liquid Downflow through Packed Beds," *Can. J. Chem. Eng.*, **61**, 158 (1983).
Santos, J. M. de, T. R. Melli, and L. E. Scriven, "Mechanics of Gas-Liquid Flow in Packed-Bed Reactors," *Ann. Rev. Fluid Mech.*, **23**, 233 (1991).
Stork, A., M. A. Latfi, G. Barthole, A. Laurent, and J. C. Charpentier, "Electrochemical Study of Liquid-Solid Mass Transfer in Packed Bed Electrodes with Upward and Downward Cocurrent Gas-Liquid Flow," *J. Appl. ElectroChem.*, **16**, 947 (1986).
Taitel, Y., and A. E. Dukler, "A Model for Predicting Flow Regime Transitions in Horizontal and Near Horizontal Gas-Liquid Flow," *AIChE J.*, **22**, 47 (1976).
Tosun, G., "A Study of Cocurrent Downflow of Nonfoaming Gas-Liquid Systems in a Packed Bed. 1: Flow Regimes: Search for a Generalized Flow Map," *Ind. Eng. Chem. Process Des. Dev.*, **23**, 29 (1984).
Weekman, V., and J. E. Myers, "Fluid Flow Characteristics of Concurrent Gas-Liquid Flow in Packed Beds," *AIChE J.*, **10**, 951 (1964).
Wu, R., M. J. McCready, and A. Varma, "Influence of Mass Transfer Coefficient Fluctuation Frequency on Selectivity and Yield in Multiphase Reactors," *Chem. Eng. Sci.*, submitted (1994).

Appendix

Derivation of three-layer finite-height K-H instability

Figure A1 shows the flow situation of interest. The three phases have different densities and velocities. Because the velocity profiles are expected to be flat and because there is only limited viscous contact between phases, Laplace's equation is expected to be valid for each phase. The experiments show that an interfacial instability occurs so that there is no density fluctuation within the phases. This simplified model will not be capable of predicting the flow rates of the phases, but if they are known, it should give a reasonably good prediction of instability. Note that the inclusion of Ergun equation force terms would allow for prediction of the base state (at least for the pure fluids), but it greatly complicates the analysis, and because all terms are resistive, the additional terms will not add to the instability. Thus the Kelvin–Helmholtz model is expected to be a lower bound on instability.

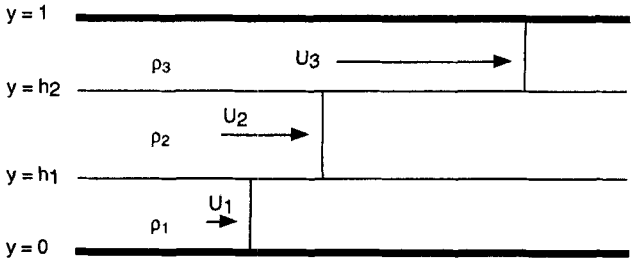

Figure A1. Three-layer flow in a packed bed.

The top layer is air, the middle layer is a bubbly phase, and the lower layer is liquid.

This analysis extends the standard Kelvin–Helmholtz analysis for a two-layer unbounded flow (Panton, 1986; Drazin and Reid, 1984) to a three-layer bounded flow. Any disturbances that are formed are assumed to be long compared to the size of a particle so that the formulation is the same as if no packing is present. A traveling interfacial disturbance is assumed to be of the form

$$\eta = a\exp[ik(x-ct)] + c.c., \tag{A1}$$

where η is the shape of the interface, a is the amplitude of the disturbance, $i=\sqrt{-1}$, k is the wave number of the disturbance scaled with the height of the channel, x is the direction of flow, t is time, and c is complex wave speed. The term $c.c.$ denotes complex conjugate. Because this is a linear problem, the conjugate does not contain any additional information and is not needed. The real part of c gives the speed of the disturbance and a positive imaginary part denotes growth. The velocity components for the three phases, $\mathbf{u}_j$, are defined from the velocity potentials, ϕ_i, as

$$\mathbf{u}_j = \nabla\phi_j, \quad i=1,2,3 \tag{A2}$$

for each of $j=1,2,3$ phases. Laplace's equation will govern the velocity potential for each phase. The normal velocity must be 0 at the top and bottom walls. If Laplace's equation is solved for the lower region, the answer is

$$\phi_1 = A_1\cosh[ky]\exp[ik(x-ct)]. \tag{A3}$$

The solution for the middle region is

$$\phi_2 = (A_2\exp[-ky] + B_2\exp[ky])\exp[ik(x-ct)], \tag{A4}$$

and the upper region is

$$\phi_3 = A_3(\exp[ky] + \exp[2k - ky])\exp[ik(x - ct)]. \quad \text{(A5)}$$

The kinematic boundary conditions for the lower interface are

$$\frac{\partial \eta_1}{\partial t} + U_j \frac{\partial \eta_1}{\partial x} = \frac{\partial \phi_i}{\partial y}, \quad j = 1,2 \quad @y = h_1. \quad \text{(A6)}$$

At the upper interface, the kinematic boundary conditions are

$$\frac{\partial \eta_2}{\partial t} + U_j \frac{\partial \eta_2}{\partial x} = \frac{\partial \phi_j}{\partial y}, \quad j = 2,3 \quad @y = h_2. \quad \text{(A7)}$$

The dynamic boundary condition for $y = h_1$ is

$$\rho_2\left(-\frac{\partial \phi_2}{\partial t} - U_2\frac{\partial \phi_2}{\partial x} - g\eta_1\right) - \rho_1\left(-\frac{\partial \phi_1}{\partial t} - U_1\frac{\partial \phi_1}{\partial x} - g\eta_1\right) - \gamma_1\frac{\partial^2 \eta_1}{\partial x^2} + \sigma_1\eta_1 = 0. \quad \text{(A8)}$$

The dynamic boundary condition for $y = h_2$ is

$$\rho_3\left(-\frac{\partial \phi_3}{\partial t} - U_3\frac{\partial \phi_3}{\partial x} - g\eta_2\right) - \rho_2\left(-\frac{\partial \phi_2}{\partial t} - U_2\frac{\partial \phi_2}{\partial x} - g\eta_2\right) - \gamma_2\frac{\partial^2 \eta_2}{\partial x^2} + \sigma_2\eta_2 = 0. \quad \text{(A9)}$$

Note that the capillary pressure term that is not a function of wave number is given by the terms that contain σ_1 and σ_2. The value used for σ is obtained from Grosser et al. (1988) as

$$\sigma_i = \frac{(1-\epsilon)}{\epsilon d_p}\sqrt{A}\,\gamma_i\frac{\partial J(\epsilon_L)}{\partial \epsilon_L}\frac{\partial \epsilon_L}{\partial y}, \quad \text{(A10)}$$

where ϵ is the bed void fraction, ϵ_L is the liquid fraction in the bed, d_p is the particle diameter, $A = 180$, the Ergun equation constant for the viscous region, γ_i is the interfacial tension in the absence of packing, and $J(\epsilon_L)$ is the Leverett drainage function given in Grosser et al. (1988). Equations A6–A9 constitute an eigenvalue problem for c. The problem was solved using a computer algebra package by successive substitution and elimination starting with the solutions for ϕ_i. The characteristic equation for c, which is too long to print here, was solved numerically.

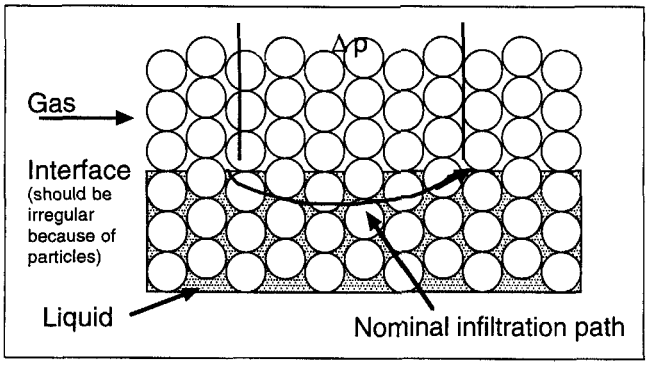

Figure A2. Gas infiltrates along the nominal path.

Pressure drop and gas momentum overcome surface tension and gravity.

Derivation pore-level force balance equation

Consider the interface region shown in Fig. A2. The interface can never be perfectly flat because of the packing; there will always be disturbances on the scale of about a particle radius. Because of this, over a fixed distance the pressure drop, Δp, will exert a force on the liquid that will try to force the liquid down in the higher pressure region (upstream) and up in the lower pressure region (downstream). The momentum of the gas flow will also force liquid out of pores because the interface is not flat. This term is written as $\rho_G U_G^2/2$ because there is an average effect of the gas over a finite region. If the angle of impingement were known, it could be included in this term. However, because it is not known, it is not included. This disturbing effect of the gas is resisted by gravity and surface tension. The force across the meniscus inside a pore caused by interfacial tension is $2\gamma/r_h$, where r_h is the radius of curvature and γ is the surface tension coefficient. The effect of gravity will be felt over the entire region. Thus the effective buoyancy force is $\epsilon\,(\rho_L - \rho_G)\,g\Delta h$. If the forces are in balance the equation is

$$-\Delta P + \frac{\rho_G U_G^2}{2} = \epsilon(\rho_L - \rho_G)g\Delta h + 2\frac{\gamma}{r_h}. \quad \text{(A11)}$$

Infiltration is predicted if the left side of Eq. A11 is larger than the right side.

Manuscript received June 3, 1994, and revision received Aug. 31, 1994.